NI-MN-GA ACTUATING ELEMENTS MANUFACTURED USING 3D PRINTING

ULLAKKO K[1], LAITINEN V[1], SAREN A[1], SOZINOV A[1], MUSIIENKO D[1], CHMIELUS M[2], SALMINEN A[1]

[1] Lappeenranta University of Technology, Finland
[2] University of Pittsburgh, USA

ABSTRACT

Laser additive manufacturing was employed to print near net shape components from gas atomised Ni-Mn-Ga powder. The heat-treated components exhibited a polycrystalline 10M martensitic structure. The magnetic-field-induced strain was measured to be 100 ppm. The results indicate that it is possible to use laser additive manufacturing to produce Ni-Mn-Ga devices that contain sections that can be strained by an external magnetic field.

KEYWORDS:MAGNETIC-FIELD-INDUCED STRAIN; MAGNETIC SHAME MEMORY EFFECT; MSM; 3D PRINTING; ADDITIVE MANUFACTURING; LASER POWDER BED FUSION; LPBF

INTRODUCTION

It was recently demonstrated that polycrystalline Ni-Mn-Ga foam-like [1] and lattice structures [2-5] can be produced by additive manufacturing using binder jetting and 3D ink-printing processes. Our goal is to employ an additive manufacturing process to produce devices such as valves and grippers from magnetic shape memory (MSM) alloys. These devices will contain single crystalline actuating parts, the dimensions of which can be changed by an external magnetic field, in combination with other parts that form the body of the device. Our modelling demonstrated that it is also possible to use laser additive manufacturing to produce single crystalline Ni-Mn-Ga components [6]. We are currently exploring the possibility of employing a laser powder bed fusion (LPBF) process to manufacture single crystalline MSM components.

LPBF uses a focused laser beam to selectively melt and fuse powder material on a layer-by-layer basis [7]. This process has been used to manufacture components from thermal shape memory alloys like Ni-Ti and Cu-Al-Ni-Mn [8-18]. Direct metal laser deposition has been used to print Ni-Co-Mn-Sn magnetocaloric materials on an experimental basis [19-20]. In the current study, LPBF was used for the first time to make near net shape polycrystalline Ni-Mn-Ga components, characterise the resulting structure and composition, and demonstrate magnetic-field-induced strains of the components.

RESULTS AND DISCUSSION

An in-house built LPBF system was used to manufacture cuboids from argon gas atomised Ni-Mn-Ga powder. The cuboids (side view shown in Fig. 1a) were manufactured in patches of three samples on stainless steel 316L substrates. The LPBF system was equipped with an IPG 200W ytterbium fibre laser with 82 µm diameter laser beam having a Gaussian power distribution focused on the surface of the powder bed. A layer thickness of 120 µm was used in the experiments due to the large maximum particle size of the powder. The cuboids were fabricated by melting numerous single tracks layer by layer on top of each other based on the DXF models. The resulting volumetric energy density for the single track process was 163 J/mm^3. The Ni-Mn-Ga samples were manufactured at room temperature, and argon was used as shielding gas.

One batch of the manufactured Ni-Mn-Ga components was homogenised at 1303 K for 48 hours and subsequently annealed at 973 K for 10 hours in an argon atmosphere. Microstructural analyses were performed for the heat-treated Ni-Mn-Ga samples using optical polarised light microscopy and X-ray diffraction (XRD). The analysis revealed that the Ni-Mn-Ga sample exhibited 10M martensitic structure. Fig. 1b shows the microstructure of an as-processed Ni-Mn-Ga sample near the sample-substrate interface. Repeated melting and solidifying of the material during the LPBF process resulted in the room temperature microstructure in which laser scan tracks were identifiable in cross-sectional profiles. Fig. 1c demonstrates the internal microstructure of a heat-treated sample, which was found to contain only polycrystalline 10M martensite. The Martensite twin variants are clearly visible in the figure. This finding is in agreement with the observations presented in [19-20]. The martensite transformation temperatures and Curie point of a heat-treated sample were determined using a low-field ac magnetic susceptibility method as A_s = 323 K, A_f = 348 K, M_s = 348 K, M_f = 318 K and T_C = 360 K.

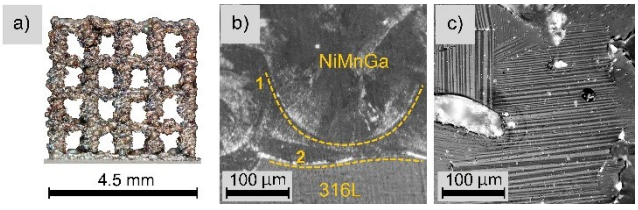

Fig.1. (a) Side view of a Ni-Mn-Ga cuboid sample manufactured by LPBF. (b) Optical image showing the microstructure of an as-processed sample near the substrate interface. Dashed lines mark: (1) cross-sectional profile of a laser scan track, and (2) fusion boundary between Ni-Mn-Ga and the 316L substrate. (c) Internal microstructure of a heat-treated sample demonstrating martensite twin variants.

The laser Doppler vibrometry (LDV) setup described in [21] was used to measure the contraction of the sample during magnetic field actuation, with a temporal resolution

of 0.2 µs. The magnetic field source was a 16 mm length solenoid with 4 mm inner diameter, which consisted of 140 turns of 0.2 mm insulated copper wire. The solenoid was connected to a high-voltage pulse generator in series with an additional passive circuit used to square and extend the current pulse to ~80 µs. The applied magnetic field varied from 0.17 to 1.65 T. The sample was attached on one side with Loctite® Super Glue to a rigid sapphire rod. The inset in Fig. 2a shows the schematic of the experimental setup used for the pulsed magnetic field actuation. The measurement was conducted on a ladder-like pillar that was extracted from a heat-treated Ni-Mn-Ga sample. The pillar had a length of approximately 4 mm. All measurements were conducted at room temperature. The magnetic-field-induced strain of the pillar is shown in Fig. 2a. The strain was calculated from the average value of the displacement signal (as shown in Fig. 2b) at the time frame of 20-40 µs, when the field was constant. Fig. 2b shows the measured temporal dependence of the displacement of the end of the pillar (magnetic field 1.65 T). The displacement signal follows the fast current pulse and also induces vibrations in the pillar. The displacement recovered when the field was removed. As shown in Fig. 2, the pillar contracted in response to the applied magnetic field, and the strain saturated at about 1 T. The maximum strain of the pillar was measured to be 100 ppm.

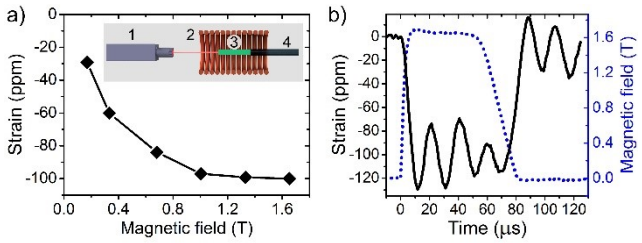

Fig.2. (a) Magnetic-field-induced strain as a function of the applied magnetic field in the pillar extracted from a heat-treated Ni-Mn-Ga sample. The inset shows a schematic view of the LDV measurement setup. The labelled parts are as follows: (1) laser head, (2) solenoid, (3) Ni-Mn-Ga sample, (4) sapphire rod. (b) The strain (left axis, solid black line) and the magnetic field strength (right axis, blue dotted line) versus time recorded for the 1.65 T magnetic field pulse, corresponding to the rightmost point in (a).

CONCLUSION

In conclusion, a laser powder bed fusion process was used for the first time to produce near net shape Ni-Mn-Ga components from gas atomised powder. X-ray diffraction measurements revealed a mixture of polycrystalline austenitic and 10M martensitic structure in the as-processed samples, and polycrystalline 10M Martensitic structure in the heat-treated samples. The components were shown to strain 100 ppm by an applied magnetic field. The experiment also demonstrated that actuating Ni-Mn-Ga components can be built on dissimilar materials, thus enabling Ni-Mn-Ga-based hybrid structures. The reported results represent an important step forward in the efforts to use laser additive manufacturing approaches to produce MSM devices.

Project was supported by the Strategic Research Council (SRC) of Finland (Grant No. 313349) and the Academy of Finland (grant number 287016).

REFERENCES

[1] A. Mostafaei, K. Kimes, E. Stevens, J. Toman, Y. Krimer, K. Ullakko, M. Chmielus, Acta Mater. 131 (2017) 482-490.
[2] M.Caputo, C. Solomon, Microsc. Microanal. 23 (2017) Suppl 1.
[3] M. Caputo, C. Solomon, Mater. Letters. 200 (2017) 87-89.
[4] S. Taylor, R. Shah, D. Dunand, Acta Mater. 143 (2018) 20-29.
[5] M. Caputo, A. Berkowitz, A. Amstrong, P. Müllner, C. Solomon, Additive Manuf. Accepted manuscript (2018) https://doi.org/10.1016/j.addma.2018.03.028
[6] K. Ullakko, A. Sozinov, J. Järvinen, Proc. of Int. Conf. FSMA 2016, Sendai, Japan, Sept 2016
[7] I. Gibson, D. Rosen, B. Stucker, Additive Manufacturing Technologies, second ed., Springer, New York, 2010.
[8] I. Shishkovsky, I. Yadroitsev, I. Smurov, Phys. Procedia. 39 (2012) 447-454.
[9] J. Walker, M. Elahinia, C. Haberland, ASME 2013 Conf. on Smart Mater. (2013) V001T01A007. doi:10.1115/SMASIS2013-3074
[10] S. Dadbakhsh, B. Vrancken, J. Kruth, J. Luyten, J. Van Humbeeck, Mater. Sci. and Eng.: A. 650 (2016) 225-232.
[11] S. Saedi, A. Turabi, M. Andani, C. Haberland, H. Karaca, M. Elahinia, J. of Alloys Compd. 677 (2016) 204-210.
[12] S. Saedi, A. Turabi, M. Andani, C. Haberland, M. Elahinia, H. Karaca, Smart Mater. Struct. 25 (2016) 035005.
[13] R. Hamilton, B. Bimber, M. Taheri Andani, M. Elahinia, J. of Mater. Process. Technol. 250 (2017) 55-64.
[14] M. Elahinia, N. Shayesteh Moghaddam, A. Amerinatanzi, S. Saedi, G. Toker, H. Karaca, G. Bigelow, O. Benafan, Scr. Mater. 145 (2018) 90-94.
[15] S. Saedi, N. Shayesteh Moghaddam, A. Amerinatanzi, M. Elahinia, H. Karaca, Acta Mater. 144 (2018) 552-560.
[16] X. Wang, M. Speirs, S. Kustov, B. Vrancken, X. Li, J. Kruth, J. Van Humbeeck, Scr. Mater. 146 (2018) 246-250.
[17] J. Sam, B. Franco, J. Ma, I. Karaman, A. Elwany, J. Mabe, Scr. Mater. 146 (2018) 164-168.
[18] T. Gustmann, A. Neves, U. Kühn, P. Gargarella, C. Kiminami, C. Bolfarini, J. Eckert, S. Pauly, Addit. Manuf. 11 (2016) 23-31.
[19] E. Stevens, J. Toman, K. Kimes, V.A. Chernenko, A. Wojcik, W. Maziarz, M. Chmielus, Microsc. Microanal. 22 (2016) 1774-1775.
[20] E. Stevens, K. Kimes, V. Chernenko, A. Wojcik, W. Maziarz, J. Toman, M. Chmielus, Proceedings of Conf. Mater. Sci. & Tech. (2017) 430-432.
[21] A. Saren, D. Musiienko, A.R. Smith, K. Ullakko, Scr. Mater. 113 (2016) 154-157.